


Article

Hydrochemical Characteristics and Irrigation Suitability Evaluation of Groundwater with Different Degrees of Seawater Intrusion

Zhenyan Wang ^{1,2}, Shu Wang ^{1,2}, Wenyue Liu ¹, Qiao Su ² , Hui Tong ¹, Xingyong Xu ^{2,*}, Zongjun Gao ¹ and Jiutan Liu ¹

¹ College of Earth Science and Engineering, Shandong University of Science and Technology, Qingdao 266590, China; 201882030051@sdust.edu.cn (Z.W.); wssdust@126.com (S.W.); lwysdust@126.com (W.L.); thsdust@126.com (H.T.); zongjungao1964@163.com (Z.G.); ljtsdust@126.com (J.L.)

² Key Laboratory of Marine Sedimentology and Environmental Geology, First Institute of Oceanography, Ministry of Natural Resources, Qingdao 266061, China; suqiao@fio.org.cn

* Correspondence: xuxingyong@fio.org.cn

Received: 21 October 2020; Accepted: 7 December 2020; Published: 9 December 2020



Abstract: Groundwater in coastal aquifers is often affected by seawater intrusion, resulting in water quality deterioration. Using groundwater influenced by seawater intrusion for irrigation can lead to crop failure, erosion of machinery and pipes, and adverse effects on farming. In this study, the results of water testing, methods of statistical analysis, ion ratios, a Piper diagram, and a variety of groundwater irrigation suitability models were used to analyze the chemical composition of groundwater and the influence of seawater intrusion. The result shows that the content of Na^+ , K^+ , Ca^{2+} , Mg^{2+} , Cl^- , and SO_4^{2-} in groundwater would increase due to seawater intrusion, and the increasing trend was consistent with the freshwater–seawater mixing line. With the deepening of seawater intrusion, the hydrochemical type gradually changes from $\text{Ca-HCO}_3\text{-Cl}$ to Na-Mg-Cl-SO_4 and then to Na-Cl type, and the source of hydrochemical composition changes from “Rock Weathering Dominance” to “Evaporation Dominance”. When the Cl^- concentration is greater than 7.1 meq/L, groundwater will corrode pipelines and instruments; when greater than 28.2 meq/L, excessively high salinity of groundwater will have adverse effects on planting; and when greater than 14.1 meq/L, the groundwater hardness is too high, which may make the groundwater unsuitable for cultivation.

Keywords: seawater intrusion; groundwater; hydrochemistry; irrigation suitability; Laizhou Bay

1. Introduction

Groundwater is an important part of the water cycle and the main source of water in many parts of the world [1–3]. Whether groundwater is suitable for use depends on its quality, and the quality of groundwater varies around the world due to different geology, climate, structure, topography, and other conditions [4–6]. The chemical composition and quality of groundwater may change under the influence of climate change, geological hazards, and human activities [7–9]. In coastal areas, due to the change in groundwater hydrodynamic conditions, the process of seawater invaded into freshwater aquifers on land is called seawater intrusion [10]. Seawater intrusion can be generally divided into two categories according to its formation cause, invasion route, and occurrence process: The first is the impact of various natural factors (such as climate change or sea level rise) and human factors (mainly excessive groundwater exploitation), which causes seawater to invade the coastal freshwater aquifer through the groundwater system, and generally occurs relatively slowly, causing a gradual disaster; the other type mainly occurs in estuarine areas, through the ocean surface, upstream invasion along the river, especially affected by storm surge, sea flow, tide, current, wind direction, and wind

speed and other factors, and generally occurs more suddenly, causing a sudden disaster [11–13]. Seawater intrusion will cause great changes in the chemical composition of groundwater, resulting in a series of environmental geological problems, such as salinization of freshwater, salinization of soil, and deterioration of water quality [14,15].

It is common for coastal aquifers around the world to be affected by seawater intrusion. As a result, seawater intrusion has drawn extensive attention from the international community, and relevant countries have been actively engaged in the research and treatment of seawater intrusion [16,17]. Internationally, the study of seawater intrusion began in the late 19th century: the establishment of Ghyben–Herzberg’s hydraulic equilibrium theory at the interface of brackish and freshwater is a sign that seawater intrusion enters the stage of quantitative analysis [18]. After the first International Conference on seawater intrusion was held in Hanover, Germany in 1968, seawater intrusion has become a hot research issue in the field of geoscience and water science. So far, dozens of countries and regions have studied seawater intrusion, such as the United States, Netherlands, South Korea, Japan, China, and so on. In recent years, research on seawater intrusion has mainly focused on numerical simulation, the impact of climate change on seawater intrusion, and the prevention and control methods of seawater intrusion; for example, the authors of [19], using laboratory experiment and numerical simulation methods, studied the effect of aquifer recharge and flow barriers on seawater intrusion and found that recharging the toe of the saltwater wedge was more effective in preventing seawater intrusion; the authors of [20] studied the seawater intrusion of the Nile Delta aquifer under climate change conditions and found that the rise of sea level has a significant effect on seawater intrusion; the authors of [21] used an analytical solution to study the effect of aquifer slope on seawater intrusion and found that aquifers thin towards the sea are most susceptible to sea level rise and seawater intrusion.

The research on seawater intrusion in China began in the 1970s. The background of the research is the excessive exploitation of groundwater in the Bohai Rim area, and the seawater intrusion in Dalian, Qinhuangdao, Shouguang, Laizhou, Longkou, and other places occurred to different degrees. Seawater intrusion directly leads to the gradual deterioration of the groundwater environment and the decrease of groundwater applicability, the abandonment of a large number of mechanical Wells and civilian Wells, and the shortage of limited underground freshwater resources. Since the phenomenon of seawater intrusion such as salty water quality and increased Cl^- concentration was found in Shouguang, Hanting, Laizhou, and other regions in 1970s, Laizhou Bay has become a key area for the study of seawater intrusion in China. In recent years, many scholars have studied the seawater intrusion in Laizhou Bay; for example, the authors of [22] investigated the seawater intrusion of the southern coast of Laizhou Bay and found that the degree of saline water intrusion in Holocene groundwater is more serious than that in Late Pleistocene groundwater; the authors of [23] studied the fluorine in the groundwater of southern coast of Laizhou Bay and suggested that the seawater intrusion led to the release of more F into the groundwater from rocks and soil; the authors of [24] applied H, O, and Li isotopes to study the groundwater of the southern coast of Laizhou Bay and suggest that shallow saline groundwater originated from brine diluted with seawater and fresh groundwater, and deep saline groundwater originated from seawater intrusion. The influence of groundwater on agricultural cultivation has also been widely concerned by scholars. The authors of [25] improved an index for evaluating the suitability of groundwater for agricultural planting and applied it in Al Kufa region, suggesting that the groundwater in this region is suitable for agricultural irrigation; the authors of [26] studied the changes of water quality in South Korea over the years and evaluated the suitability of irrigation using various models, suggesting that the groundwater in this area was suitable for agricultural irrigation. Compared with using a single model to evaluate the irrigation suitability of groundwater, using multiple indicators to evaluate the suitability of groundwater planting from various angles can get more comprehensive and objective results. There exist numerous studies on seawater intrusion and groundwater irrigation suitability, but there exist few combination studies. Weifang is an important agricultural production base in China, and the research area is located in the north of Weifang. This study uses the hydrogeochemical method, geological statistics method, and a

variety of agricultural irrigation evaluation model to (1) clarify the source of the chemical composition of groundwater in the southern and east-southern coast of Laizhou Bay, (2) track the changes and influencing factors of each ion component in groundwater with the deepening of seawater intrusion, and (3) evaluate the suitability of groundwater for agricultural irrigation with different degree of seawater intrusion. The results of this study are expected to provide theoretical support for future groundwater management and seawater intrusion treatment in the Laizhou Bay area and provide reference for other seawater intrusion areas in the world.

2. Study Area

2.1. Physiographic Condition

Laizhou Bay belongs to the Southern Bohai Sea, is one of the three bays in the Bohai Sea. The underwater terrain of Laizhou Bay is gentle; in most areas the water is within ten meters and the seafloor sediments are mainly silt and silt. The study area (Figure 1) is in the southern and east-southern coast of Laizhou Bay. The geographical coordinates are between 118°57' and 119°59' E and 36°40' and 37°20' N. The cities involved are Shouguang, Weifang, Changyi, Pingdu, and Laizhou, with a total area of about 4400 km². The topography of the study area is high in the south and low in the north, and the flow direction of groundwater is from south to north.

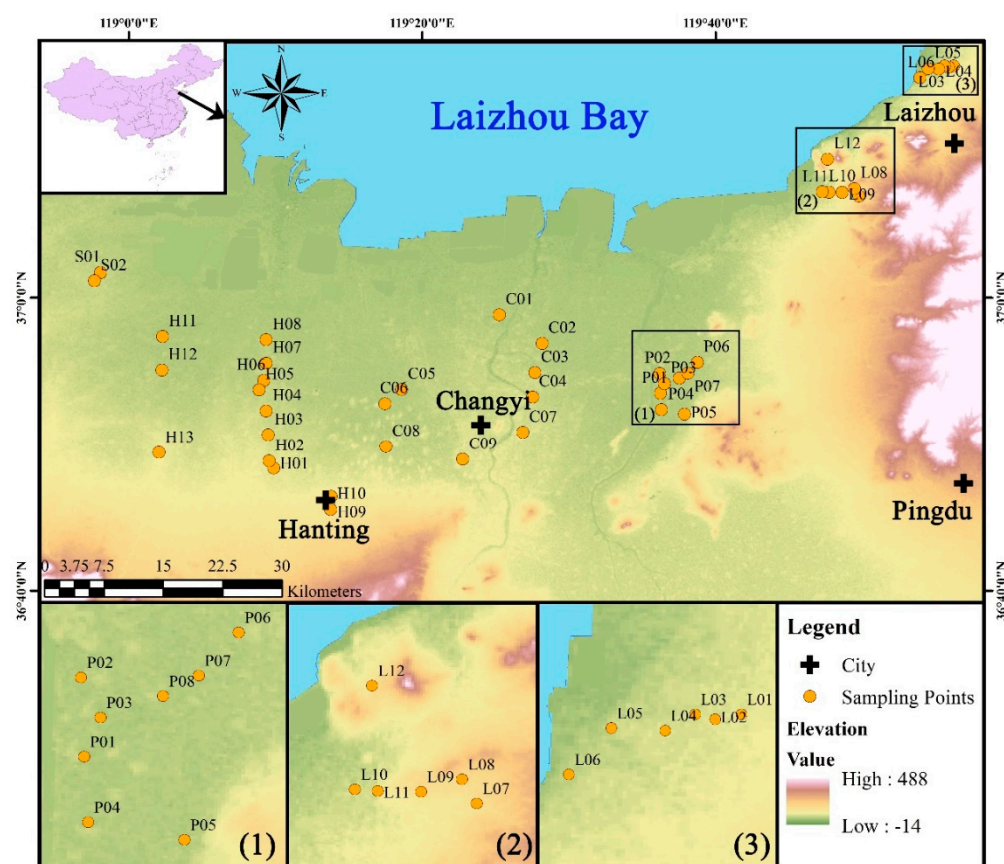


Figure 1. Location and topography of the study area and sampling points location.

The climate of the study area is a warm temperate monsoon subhumid continental climate. Influenced by the Eurasian continent and the Pacific Ocean, a monsoon climate exists, so the four seasons are distinct. The average annual temperature is 12.6 °C with cold winters and hot summers. The average annual (1971–2010) rainfall in the study area was about 660 mm, and the precipitation was mainly distributed in the rainy season from June to September. The average annual (1971–2010)

evaporation was about 1802 mm, and the rainfall was far lower than the evaporation. In the area, several rivers such as Weihe River, Bailang River, and Jiaolai River flow into Laizhou Bay, among which the largest river is Weihe River, with an average annual flow of $1.5 \times 10^8 \text{ m}^3/\text{a}$; its flow rate is changed by seasons, so groundwater has become the main irrigation water source in the study area. With the development of urbanization, the proportion of impervious surface has been increasing year by year, rising from 11% in 2000 to 13% in 2010 and 20% in 2020 (Figure 2), which means a greater population and more water resource consumption in the region. In contrast, the proportion of cropland has been declining year by year, from 78% in 2000 to 70% in 2010 and then to 65% in 2020 (Figure 2). However, agriculture is the main driving force of economic and social development in the area, and how to maintain crop yield under such conditions has become a problem that the local people have to face.

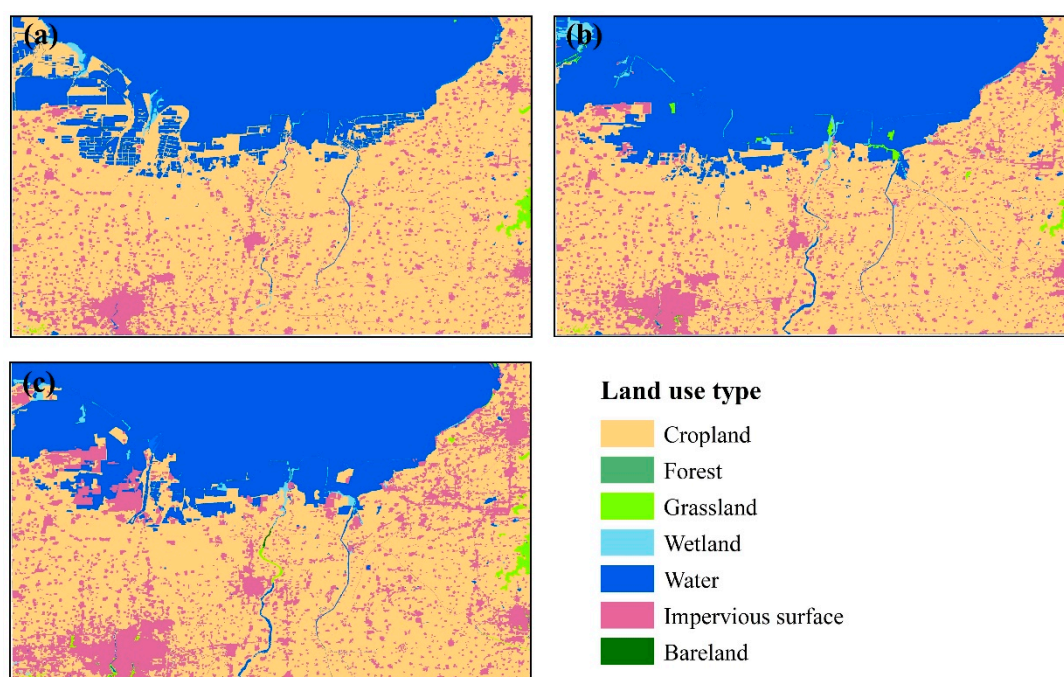


Figure 2. Land use types of the study area in (a) 2000, (b) 2010, and (c) 2020. Data were obtained from “the global land cover data products and services website of the national center for basic geographic Information (DOI: 10.11769)”.

2.2. Hydrogeology

From south to north, the study area consists of a transition of gently dipping alluvial-diluvial plain, alluvial-marine plain, and marine sedimentary plain, with the altitude decreasing from 30 m to 1–2 m. The coast of this section is silty and silty, and the quaternary sediments are relatively thick, generally ranging from 200 to 300 m (Figure 3). The alluvial plain in the region is composed of multiple alluvial fan groups of the adjacent fan margin. The leading edge of the alluvial plain is buried by marine deposits of alluvial deposits of the Yellow River. The aquifer has a large thickness and coarse grain and has a multilayer structure, which shows the trend of the grain changing from coarse to fine from bottom to top in a vertical direction. The southern and east-southern coast of Laizhou Bay is mainly distributed in loose pore aquifers, and the water inflow from a single well in most areas is 1000–3000 m^3/d . The bedrock fissure aquifer is mainly distributed in Laizhou and flat hilly areas, with a small water inflow of about 100 m^3/d .

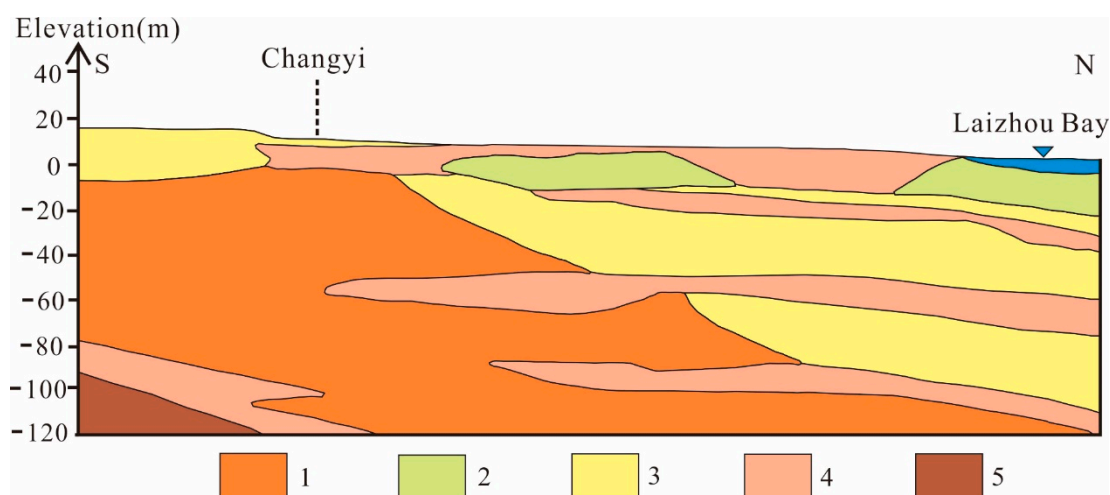


Figure 3. Hydrogeological section of the southern coast of Laizhou Bay. (1) Gravel and sand. (2) Middle and fine sand. (3) Clayey sand. (4) Silt and clay. (5) Basalt and andesite of Neogene.

3. Materials and Methods

3.1. Sampling and Testing

In this study, groundwater samples were collected from 45 wells in use on the southern and east-southern coast of Laizhou Bay in November 2019. The sampling locations are shown in Figure 1, and seawater samples were collected in Laizhou Bay in November 2018. The electric conductivity, TDS, pH, and other parameters of the groundwater sample were measured in the field using YSI Professional Plus, a portable water quality analyzer manufactured by YSI. Then, the groundwaters sample were collected and stored in polyethylene bottles. Before sampling, the sampling bottle is thoroughly cleaned with well water three times. When sampling, we fill the whole bottle and then seal the bottle with tape. The samples were collected, stored, and transported in strict accordance with the technical specifications for groundwater environmental monitoring.

The contents of Ca^{2+} , Mg^{2+} , Na^+ , K^+ , Cl^- , SO_4^{2-} , HCO_3^- , and Br^- in all samples were determined in the laboratory. The Na^+ and K^+ ions were determined by flame atomic absorption spectrophotometry with a detection limit of 2.0 mg/L. The instrument was an atomic absorption spectrophotometer. Ca^{2+} and Mg^{2+} were determined by EDTA titration. The detection limit was 0.01 mg/L. HCO_3^- , which was determined by acid–base indicator titration, and the detection limit was 1.0 mg/L. SO_4^{2-} , Cl^- , and Br^- , which were detected by ion chromatography with corresponding detection limits of 0.09 mg/L, 0.02 mg/L, and 0.1 mg/L, respectively, and the instrument used was an ion chromatograph ICS-2100 produced by the DIONEX company in the United States.

3.2. Analytical Methods

The maximum, minimum, average, and coefficient variation (CV) of each parameter were calculated, and the main ion boxplot was drawn with Origin. A Piper diagram is a graph commonly used in hydrogeochemical analysis [27], it directly reflects the hydrochemical characteristics by the main percentage of anion and anion milligram equivalent. A Gibbs diagram is a graph utilized to determine the source of the chemical composition of water [28]. Based on the analysis of the chemical composition of global precipitation, river, lake, and ocean water, Gibbs believes that atmospheric precipitation, rock weathering, and the evaporation–crystallization process are the three hydrochemistry controlling factors of global water [29,30].

The geostatistical method used in this study is ordinary kriging, which is a commonly used kriging interpolation method. The essence of the kriging interpolation method is to make an unbiased and optimal estimation of the parameters of unknown points by using the relevant parameters of known points and the structural characteristics of the variation function. Compared with other interpolation methods, the remarkable characteristic of the kriging interpolation method is the minimum variance of error. In this study, the Kriging module in ArcGis was used and the call path is ArcMap-ArcToolbox-Spatial Analyst Tools-Interpolation-Kriging.

End-member mixing is a process involving selecting fresh water and seawater as two end-members and then, based on mass balance, the two end-members are mixed in proportion. A mixing line based on different mixing proportion points is drawn to help analyze the process of groundwater and seawater mixing:

$$C_m = C_s \times X + C_f \times (1 - X) \quad (1)$$

where C_m represents the concentration of each component in the mixed solution, C_s represents the concentration of each component in seawater, C_f represents the concentration of each component in freshwater, and X represents the mixing proportion of seawater. Through setting different X values, the mixing line between seawater and groundwater can be obtained.

In this study, water quality evaluation models were used to evaluate the suitability of groundwater for agricultural irrigation in the study area, including the sodium adsorption ratio (SAR), percentage sodium (%Na), corrosivity ratio (CR), residual sodium carbonate (RSC), and total hardness (TH). Their respective calculation methods and standard division are shown in Table 1.

Table 1. Evaluation models and classification criteria for irrigation suitability.

Indicator	Equation	Range	Classification	Reference
SAR	$SAR = \frac{Na^+}{\sqrt{\frac{Ca^{2+} + Mg^{2+}}{2}}}$	<10	Excellent	[31]
		10–18	Good	
		18–26	Doubtful	
		>26	Unsuitable	
%Na	$\%Na = \frac{Na^+ + K^+}{Ca^{2+} + Mg^{2+} + Na^+ + K^+}$	<20	Excellent	[32]
		20–40	Good	
		40–60	Permissible	
		60–80	Doubtful	
CR	$CR = \frac{(Cl^- / 35.5) + 2(SO_4^{2-})}{(CO_3^{2-} + HCO_3^-) / 50}$	>80	Unsuitable	[33]
		≤1	Non-corrosive	
		>1	Corrosive	
RSC	$RSC = (CO_3^{2-} + HCO_3^-) - (Ca^{2+} + Mg^{2+})$	<1.25	Safe	[31]
		1.25–2.5	Marginally suitable	
		2.5–5	Unsuitable	
		>5	Harmful	
TH	$TH = 2.597Ca^{2+} + 4.115Mg^{2+}$	<75	Soft	[2]
		75–150	Moderately hard	
		150–300	Hard	
		>300	Very hard	

4. Results

4.1. Statistical Analysis

The testing results are shown in Table A1. The boxplot (Figure 4) showed that the main cation sequence of groundwater was $\text{Na}^+ > \text{Ca}^{2+} > \text{Mg}^{2+} > \text{K}^+$. Among these ions, the dominant cation is Na^+ , the maximum value of Na^+ is 1643.1 mg/L, the minimum value is 37.73 mg/L, and the mean value is 405.1 mg/L (Table 2). The content span of Na^+ is large, and the CV reaches 0.98, indicating its strong spatial dispersion. Combined with the geographical location of the study area, it is believed that the groundwater in the study area is affected by seawater intrusion, leading to a rapid increase of Na^+ content within a short distance. The Ca^{2+} content occupies the second most dominant cation, with a maximum value of 596.93 mg/L, a minimum value of 32.33 mg/L, and a mean value of 183.75 mg/L. The maximum point of Ca^{2+} is H08, which is also the point with the highest Na^+ content. The Ca^{2+} content of H08 is higher than that of seawater and freshwater, indicating that the Ca^{2+} content of this point is not only from mineral dissolution and seawater but also may be affected by evaporation and cation exchange. The Mg^{2+} content ranged from 18.23 to 271.6 mg/L, and the mean value was 91.3 mg/L, both of which were far lower than the 785.5 mg/L of seawater. The highest Mg^{2+} content was P04, which was also the second highest Cl^- content. The high Mg^{2+} content may be influenced by seawater. K^+ contains the least amount of main cations in the groundwater, with a range of 0.68 to 46.96 mg/L and a CV as high as 1.3, indicating its strong spatial dispersion. Due to the similar physical and chemical properties of K^+ and Na^+ , it is believed that K^+ is also affected by seawater. The main anion sequence of groundwater was $\text{Cl}^- > \text{HCO}_3^- > \text{SO}_4^{2-}$. The Cl^- concentration range is 87.1 to 3222.22 mg/L, the difference is over 3000 mg/L, and the difference between the minimum Cl^- concentration point and the maximum point is only about 20 km from the offshore vertical distance, indicating that the inland water is greatly affected by seawater in this distance. The content range of HCO_3^- is 152.34 to 999.33 mg/L, and its CV is small, indicating poor spatial dispersion, and the main source may be mineral dissolution. The content of SO_4^{2-} ranged from 52.41 to 1127.08 mg/L, with an average value of 275.07 mg/L. The content of SO_4^{2-} was the highest at H08, indicating that the content of SO_4^{2-} was also affected by seawater. The TDS content of groundwater has a large span, with a minimum value of 806 mg/L and a maximum value of 7767.5 mg/L, with the difference being about 7000 mg/L. The pH distribution in the study area is relatively uniform, and the CV is only 0.03. Overall, the groundwater in the study area is weakly acidic water.

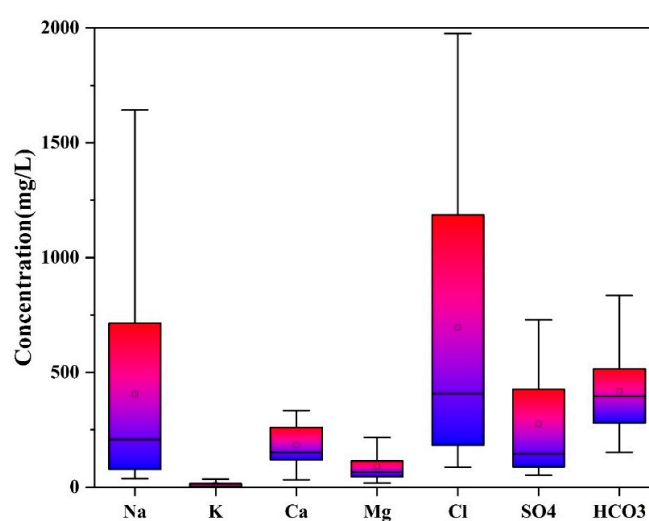


Figure 4. Boxplot of main cations and anions of groundwater in the study area.

Table 2. Statistical results of groundwater chemistry.

Parameters	Maximum	Minimum	Average	CV
Ca ²⁺	596.93	32.33	183.75	0.57
Mg ²⁺	271.60	18.23	91.30	0.73
Na ⁺	1643.10	37.73	405.10	0.98
K ⁺	46.96	0.68	9.95	1.30
Cl [−]	3222.22	87.10	696.03	0.97
SO ₄ ^{2−}	1127.08	52.41	275.07	0.94
HCO ₃ [−]	999.33	152.34	416.99	0.45
Br [−]	5.81	0.08	1.04	1.19
TDS	7767.50	806.00	2401.48	0.65
EC	10.45	0.73	2.91	0.68
pH	7.02	6.11	6.49	0.03

The units of TDS, Na⁺, K⁺, Ca²⁺, Mg²⁺, Cl[−], SO₄^{2−}, HCO₃[−], Br[−] are mg/L, and the unit of EC is ms/cm.

4.2. Status of Seawater Intrusion

There is still no unified definition standard for seawater intrusion, and most scholars take electrical conductivity (EC), total dissolved solids (TDS), and concentration of Cl[−] as the judgment basis for seawater intrusion. Based on the classification method in [34], groundwater is classified as either “Freshwater”, “Slightly saline water”, “Moderately saline water”, “Highly saline water”, “Very highly saline water”, or “Seawater”; the classed water samples are shown in Table 3, and the spatial distribution is shown in Figure 5. From freshwater to seawater, the degree of seawater intrusion gradually deepened. Classification results show that there are only one sample (C09) belongs to fresh water, which is located in the southern coast of Laizhou Bay, about 30 km away from the coastline; 14 samples were classified as slightly saline water, accounting for the highest proportion (31.82%), and they were mainly distributed in the southern coast of Laizhou Bay 27–46 km from the coastline and in the east-southern coast 6–10 km far from the coastline; 10 samples were classified as moderately saline water, accounting for 22.73%, and they were mainly distributed in the southern coast of Laizhou Bay 25–42 km from the coastline and in the east-southern coast 2–7 km from the coastline; six samples were classified as highly saline water and they were mainly distributed among the southern coast of Laizhou Bay 23–33 km from the coastline; 13 samples were classified as very highly saline water, accounting for 29.54%, and distributed among the southern coast of Laizhou Bay 18–35 km from the coastline. No sample belonging to the seawater classification was collected in this sampling.

Table 3. Classification and corresponding standards of seawater intrusion.

Classification	Cl [−] (meq/L)	TDS (mg/L)	EC (μs/cm)	Sample ID	(%)
Freshwater	<2.8	0–500	<700	C09	2.27
Slightly saline water	2.8–7.1	500–1500	700–2000	C04,C07,H01,H03,H04,H09,H10,H13,L01,L02,L07,L08,L11,L12	31.82
Moderately saline water	7.1–14.1	1500–7000	2000–10,000	C08,H02,H06,L03,L04,L06,L09,L10,P06,P08	22.73
Highly saline water	14.1–28.2	7000–15,000	10,000–25,000	C02,C03,C06,L05,P02,P05	13.64
Very highly saline water	28.2–282.2	15,000–35,000	25,000–45,000	C01,C05,H05,H07,H08,H11,H12,P01,P03,P04,P07,S01,S02	29.54
Seawater	>282.2	>35,000	>45,000	-	-

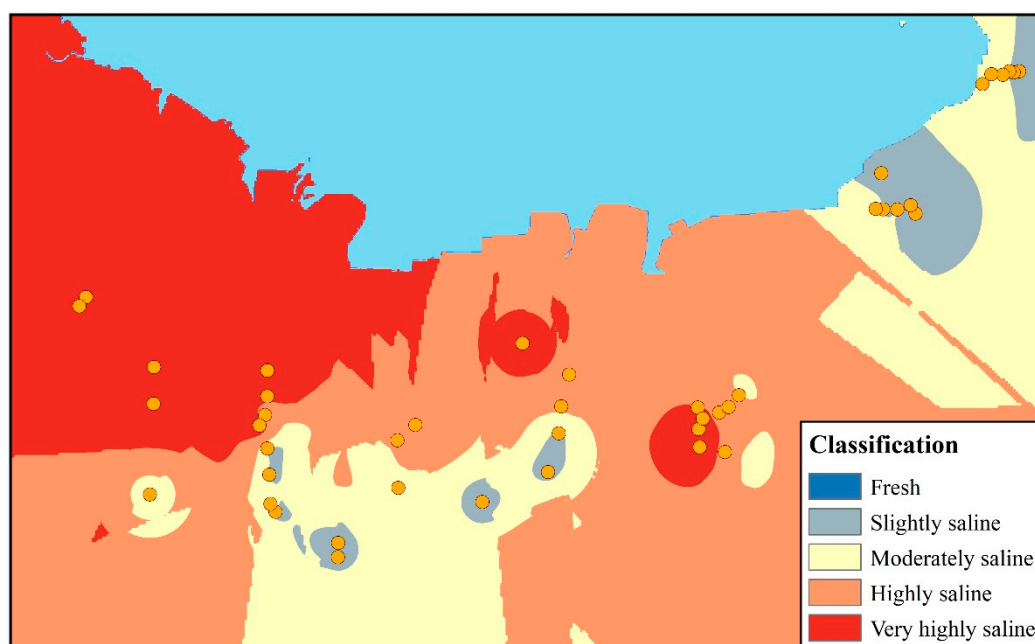


Figure 5. Spatial distribution of water samples with different degrees of seawater intrusion.

5. Discussion

5.1. Hydrochemical Type Changes with the Deepening of Seawater Intrusion

As the Piper diagram (Figure 6) revealed, freshwater belongs to the $\text{Ca}\cdot\text{HCO}_3\cdot\text{Cl}$ type; slightly saline water is mainly of $\text{Ca}\cdot\text{Mg}\cdot\text{HCO}_3\cdot\text{Cl}$ and $\text{Ca}\cdot\text{Mg}\cdot\text{Cl}\cdot\text{HCO}_3$ type; moderately saline water hydrochemical types are complicated, including $\text{Ca}\cdot\text{Cl}$, $\text{Ca}\cdot\text{Na}\cdot\text{Cl}$, and $\text{Na}\cdot\text{Cl}\cdot\text{SO}_4$; highly saline water is mainly of $\text{Na}\cdot\text{Mg}\cdot\text{Cl}$ and $\text{Na}\cdot\text{Mg}\cdot\text{Cl}\cdot\text{SO}_4$ type; very highly saline water is mainly $\text{Na}\cdot\text{Cl}$ type; seawater belongs to $\text{Na}\cdot\text{Cl}$ type. With the deepening of seawater intrusion, the hydrochemical types gradually changed from $\text{Ca}\cdot\text{HCO}_3\cdot\text{Cl}$ to $\text{Na}\cdot\text{Mg}\cdot\text{Cl}\cdot\text{SO}_4$ and then to $\text{Na}\cdot\text{Cl}$ type. The hydrochemical type of seawater is $\text{Na}\cdot\text{Cl}$ type. As the content of Na^+ and Cl^- in seawater is much higher than that of other ions in fresh groundwater, with the increase of seawater proportion, the hydrochemical type of groundwater gradually draws closer to $\text{Na}\cdot\text{Cl}$, which also exists in studies in other parts of the world [35,36].

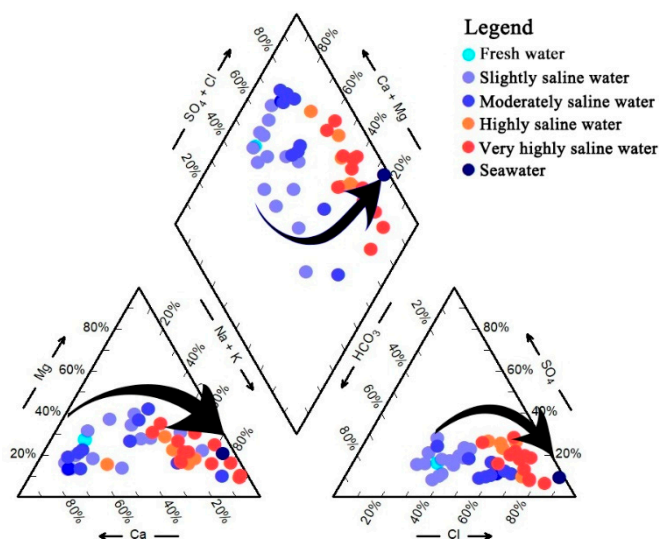


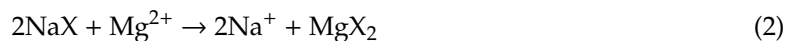
Figure 6. Piper diagram of groundwater.

As the triangular chart at the bottom left of the Piper diagram revealed, the proportion of Ca^{2+} in the cations of freshwater ranges from 80% to 60%, that in slightly saline water ranges from 60% to 20%, and that in highly saline water ranges from 30% to 20%, with the intensification of seawater intrusion, the proportion of Ca^{2+} in the groundwater presents a significant decrease trend. The proportion of Na^+ in the cations of freshwater ranges from 10% to 40%, that in slightly saline water ranges from 20% to 60%, and that in highly saline water ranges from 40% to 70%. Contrary to the trend of Ca^{2+} , the proportion of Na^+ gradually increases with the deepening of seawater intrusion. The proportion of Mg^{2+} in groundwater remains within the range of 10% to 40%. With the deepening of seawater intrusion, the proportion of magnesium ions in groundwater presents a trend of first increasing and then decreasing. As the proportion of Na^+ in seawater is much higher than that of Ca^{2+} and Mg^{2+} , the proportion of Na^+ in groundwater will gradually increase with the increase of the mixing proportion of seawater, while the proportion of Mg^{2+} and Ca^{2+} will gradually decrease. However, seawater intrusion is not an ideal mixture of seawater and underground freshwater, and water–rock interaction happens in the aquifer, resulting in changes in the ion content in the groundwater, which can explain the rising trend of the proportion of Mg^{2+} [37]. Moreover, in the process of seawater intrusion, the influence of water–rock interaction on the proportion of cations in groundwater is less than that of mixing. Therefore, as the degree of seawater intrusion deepens, the cations in groundwater will still be dominated by Na^+ .

As the triangular chart at the bottom right of the Piper diagram revealed, with the deepening of seawater intrusion, the proportion of Cl^- in the groundwater gradually increases from 25 to 50% of slightly saline water to 60 to 90% of very highly saline water, and the proportion of HCO_3^- continuously decreases from 30 to 60% of slightly saline water to 10 to 30% of very highly saline water. The proportion of SO_4^{2-} is not strongly correlated with the degree of seawater intrusion, and the SO_4^{2-} of groundwater varies within the range of 10 to 30% at each degree of seawater intrusion. In seawater, Cl^- usually occupies the highest proportion, while in fresh groundwater, HCO_3^- usually occupies the highest proportion [38]. As the Cl^- concentration in seawater is much higher than that of HCO_3^- in fresh groundwater, with the deepening of seawater intrusion, the proportion of Cl^- in groundwater will gradually increase while that of HCO_3^- will gradually decrease [39].

5.2. Variation Trends of Groundwater Ions

As shown in Figure 7, with the increase of Cl^- content, Na^+ content also gradually increased, and was distributed near the mixing line, showing a linear growth trend. With the deepening of the influence of seawater on groundwater, Mg^{2+} content in groundwater also presents a trend of a gradual increase, and its growth trend is similar to the slope of the mixing line, but the distribution of water samples is lower than the mixing line, which indicates that Mg^{2+} is influenced by other effects besides the mixing of seawater and groundwater, and water–rock interactions in aquifers may reduce the content of Mg^{2+} [40]. It may be that cation exchange in groundwater causes the decrease of Mg^{2+} in groundwater (Equation (2)):



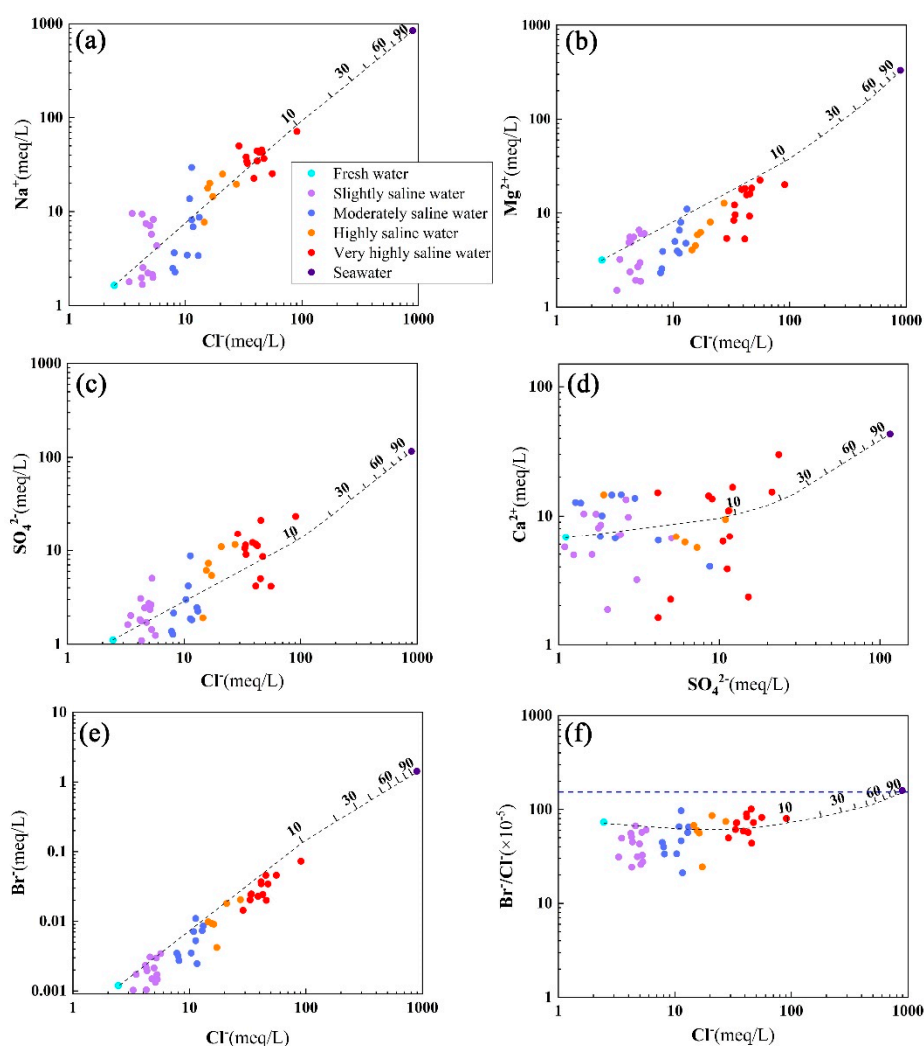


Figure 7. Hydrochemical relationships between selected ions in the groundwater and seawater composition. (a) Cl vs. Na; (b) Cl vs. Mg; (c) Cl vs. SO_4 ; (d) SO_4 vs. Ca; (e) Cl vs. Br; (f) Cl vs. Br/Cl. The black line of dashes represents the fresh–seawater mixing line, and the blue line of dashes represents the Br/Cl value of seawater.

The content of SO_4^{2-} in groundwater also increases with the increase of Cl^- content, which is consistent with the mixing line, indicating that SO_4^{2-} in groundwater mainly comes from seawater. On the whole, Ca^{2+} also tends to increase with the deepening of seawater intrusion, but most of the points fall below the mixing line, and the low Ca^{2+} content may also be affected by cation exchange (Equation (3)). The content of Br^- in freshwater is rare, but the content of Br^- in seawater is high, so Br^- is often used as an indicator parameter to judge whether groundwater is affected by seawater [41,42]. Br^- content and Br^-/Cl^- increased linearly with the increase of Cl^- content and were consistent with the mixing line. The Br^-/Cl^- value of groundwater gradually drew closer to the Br^-/Cl^- value of seawater ($\sim 1.5 \times 10^{-3}$), indicating that seawater intrusion was the main reason for the increase of groundwater Cl^- and seawater intrusion had a huge impact on the chemical composition of groundwater [43].

With the deepening of seawater intrusion, the range of Na^+/Cl^- gradually draws closer to the mixing line, indicating that seawater has an increasingly more significant influence on the chemical composition of groundwater (Figure 8). $\text{SO}_4^{2-}/\text{Cl}^-$ and $\text{Ca}^{2+}/\text{SO}_4^{2-}$ tend to decrease with the increase of Cl^- , the changing trend of $\text{SO}_4^{2-}/\text{Cl}^-$ is consistent with the mixing line, but $\text{Ca}^{2+}/\text{SO}_4^{2-}$ gradually moves away from the mixing line with the increase of Cl^- content. The explanation for this situation is that cation exchange reduces the content of Ca^{2+} in groundwater, which leads to a corresponding

decrease of $\text{Ca}^{2+}/\text{SO}_4^{2-}$. With the deepening of seawater intrusion, gypsum is precipitated before rock salt saturation, and the increasing rate of SO_4^{2-} concentration is lower than Cl^- , which leads to a gradual decrease in $\text{SO}_4^{2-}/\text{Cl}^-$ [44,45]. $\text{Mg}^{2+}/\text{Ca}^{2+}$ also increased with the increase in Cl^- content, and its trend was similar to the mixing line, but when the degree of seawater intrusion reaches “Very highly saline water”, $\text{Mg}^{2+}/\text{Ca}^{2+}$ is higher than the mixing line; the reason is that the growth rate of Ca^{2+} is slower than Mg^{2+} . On the one hand, the content of Mg^{2+} provided by seawater is higher than that of Ca^{2+} ; on the other hand, the ability of rock–soil particles to combine with Ca^{2+} is stronger than that of Mg^{2+} , and Ca^{2+} is more adsorbed in rock–soil than Mg^{2+} , and the content of groundwater is correspondingly reduced [46].

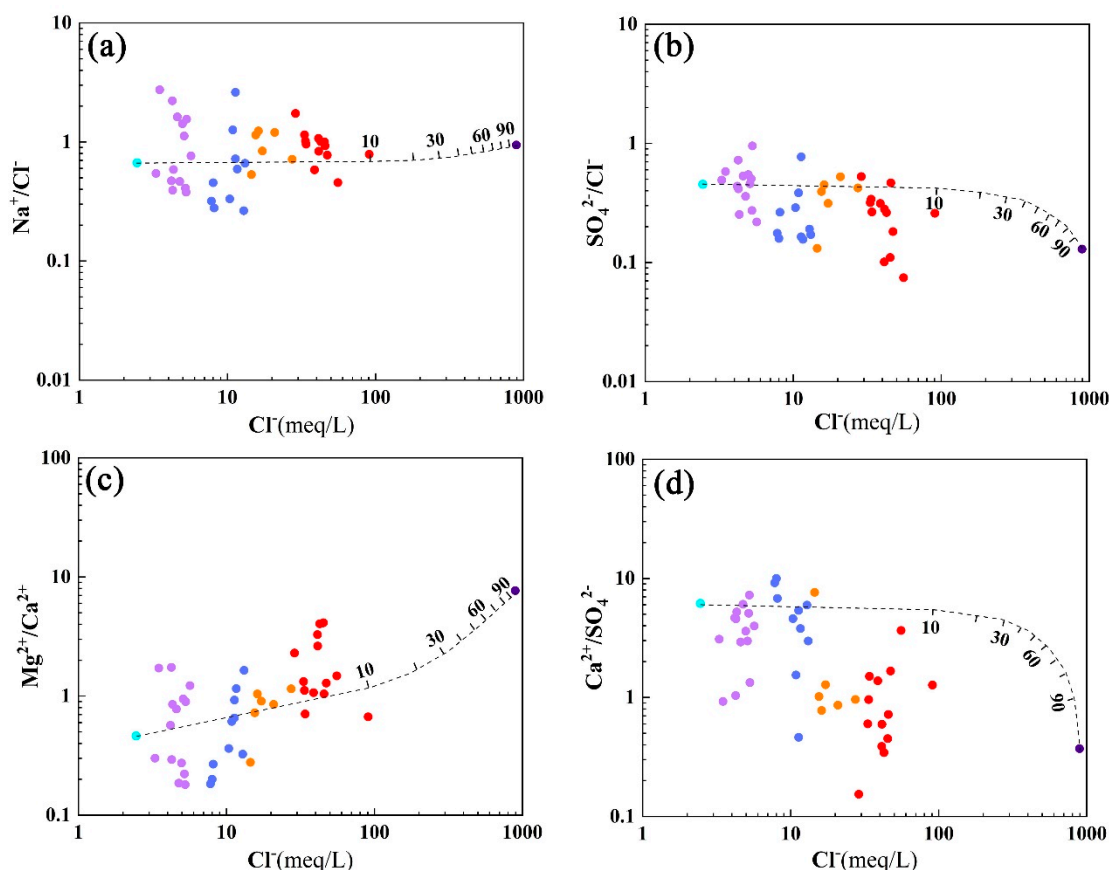


Figure 8. Evolution of hydrochemical ratios with increasing salinity. (a) Cl vs. Na/Cl ; (b) Cl vs. SO_4/Cl ; (c) Cl vs. Mg/Ca ; (d) Cl vs. Ca/SO_4 . The black line of dashes represents the fresh–seawater mixing line.

5.3. Material Sources of Groundwater

As Figure 9 revealed, the hydrochemical composition of freshwater, slightly saline water, and moderately saline water is controlled by rock weathering, that is, minerals in rocks dissolved in water are the main source of ions, and the chemical composition of freshwater, slightly saline water, and moderately saline water. However, the hydrochemical composition of highly saline water and very highly saline water are mainly evaporation dominance, which means that the process of evaporation and concentration is the major action affecting the chemical composition of highly saline water, and very highly saline water. With the deepening of the degree of seawater intrusion, the distribution of points has gradually changed from “Rock Weathering Dominance” to “Evaporation Dominance”, this means that the influence of seawater on the chemical composition of groundwater is gradually greater than that of minerals in the ground [47].

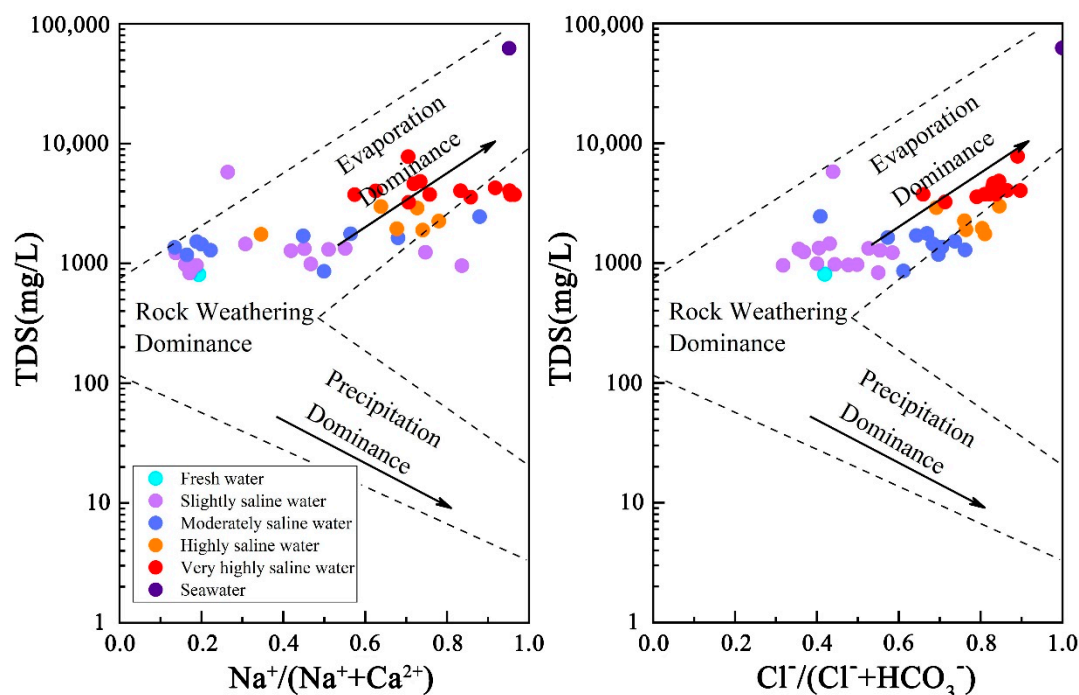


Figure 9. Gibbs diagram of groundwater in the study area.

5.4. Groundwater Evaluation for Irrigation Purpose and Its Distribution

There is already evidence that using groundwater affected by seawater intrusion reduces crop yields [48]. This study used a variety of evaluation indicators to quantify the impact of groundwater irrigation with different degrees of seawater intrusion. The results of SAR (Figure 10a) show that only two very highly saline water (C01 and C05) belongs to “Doubtful”. Four of the samples SAR values belong to “Good”, among them three samples are very saline water and one sample is moderately saline water. The SAR values of the rest of the water samples were classified as “Excellent”, indicating that only “Very Highly saline Water” has poor SAR evaluation. The results of %Na (Figure 10b) showed that the %Na values of two water samples (C01 and C05) were “Unsuitable”. Seven water samples %Na values were “Doubtful”, of which five were very highly saline water, indicating that very highly saline water might have adverse effects on planting. As both SAR and %Na show the influence of salinity on groundwater, groundwater affected by salinity may not be suitable for cultivation when the local groundwater Cl^- concentration is greater than 28.2 meq/L. As the CR result (Figure 10c) shows that most of the water samples belong to the “Corrosive” type, all the “Non-corrosive” type are slightly saline water and freshwater, it indicates that the use of fresh water and brackish water will not have adverse effects on the pipes, but when the Cl^- concentration is greater than 7.1 meq/L, it will have corrosive effects on the iron instruments and pipes. RSC results (Figure 10d) show that the majority of water samples belong to “Safe”, only one slightly saline water (H13) belong to “Marginally suitable”, indicating that the areas with low seawater intrusion may not be suitable for planting, but the possibility is low. The TH results (Figure 10e) show that only one sample (H08) TH value belongs to the “Hard”, and there are seven samples TH value belongs to “Moderately Hard”, among them six samples of seawater intrusion degree belong to “Very highly saline water”, one sample belongs to “Highly saline water”. This indicates that under the influence of seawater intrusion, the TH value of groundwater will also rise and affect planting. When Cl^- is greater than 14.1 meq/L, the TH value of groundwater may be too high for irrigation. In summary, when the Cl^- concentration is greater than 28.2 meq/L, excessively high salinity of groundwater will have adverse effects on planting. When the Cl^- concentration is greater than 7.1 meq/L, groundwater will corrode pipelines and instruments. When the Cl^- concentration is greater than 14.1 meq/L, the groundwater hardness is too high, which may make the groundwater unsuitable for irrigation.

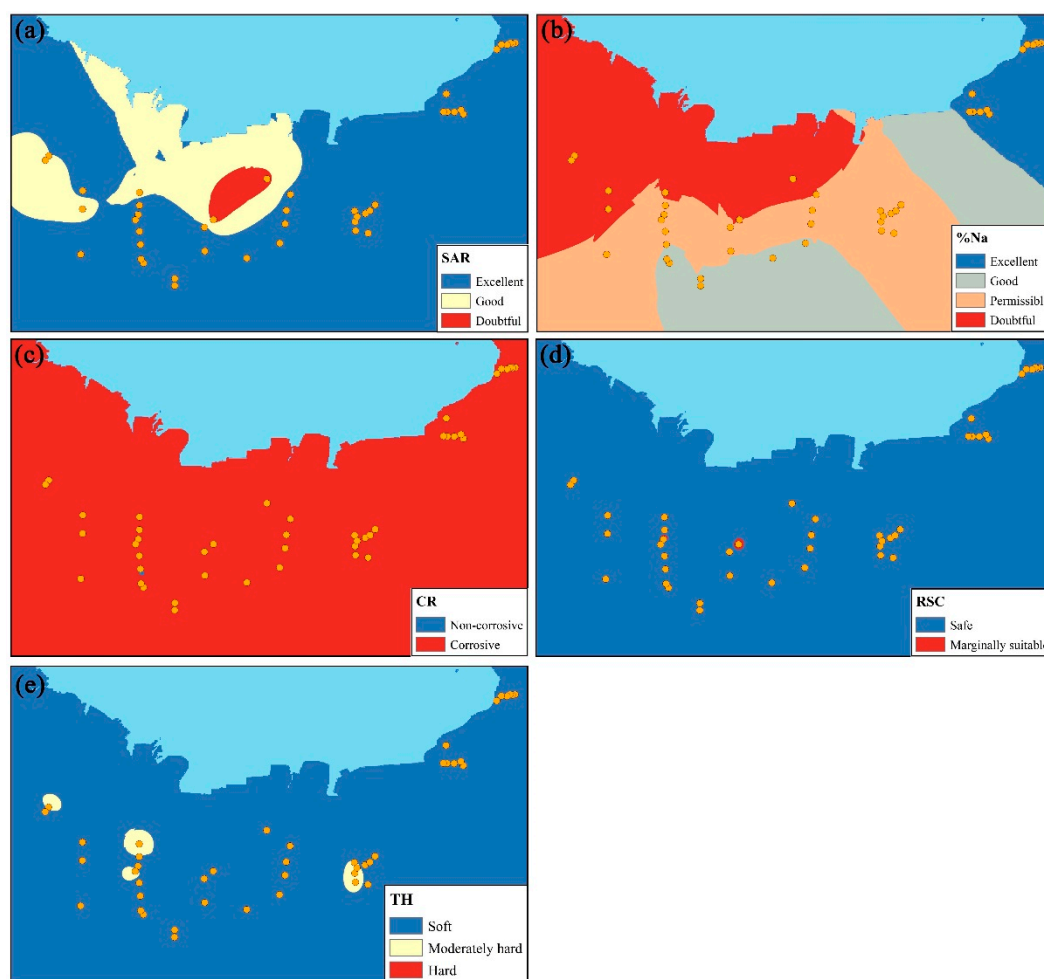


Figure 10. Evaluation results and spatial distribution of groundwater irrigation suitability. (a) SAR; (b) %Na; (c) CR; (d) RSC; (e) TH.

After being invaded by seawater, groundwater will corrode pipelines and machinery and damage infrastructure. Then, due to the increase of hardness and salinity of groundwater, crop yield will be reduced. These effects will seriously affect the development of the social economy. Therefore, measures should be taken to prevent further seawater intrusion before the Cl^- concentration in groundwater is higher than 7.1 meq/L. In the treatment of seawater intrusion, adjusting the groundwater seepage field form and cutting off the channel between seawater and land aquifer are the two main directions of seawater intrusion treatment [49,50]. No matter what method is adopted to reduce the area affected by seawater intrusion, it will be beneficial to the sustainable development of the agricultural economy in this region.

6. Conclusions

- (1) With the deepening of seawater intrusion, the contents of Na^+ , Ca^{2+} , Mg^{2+} , K^+ , Cl^- , and SO_4^{2-} in groundwater increase accordingly, and the hydrochemical type gradually changes from $\text{Ca-HCO}_3\text{-Cl}$ to Na-Mg-Cl-SO_4 and then to Na-Cl type. Seawater intrusion is not an ideal mixing process between seawater and fresh groundwater. In the process of seawater intrusion, the chemical composition of groundwater is also changing due to the constant water–rock interaction of groundwater and aquifers. However, the influence of water–rock interaction on the composition of groundwater ions is lower than that of groundwater–seawater mixing.
- (2) The chemical composition of groundwater in areas invaded by seawater is obviously affected by seawater. With the deepening of seawater intrusion, the composition of substances in

groundwater affected gradually changes from “Rock weathering dominated” to “Evaporation dominated”, showing that with the deepening of seawater intrusion, the influence of seawater on the hydrochemical composition of groundwater gradually exceeds that of mineral dissolution.

- (3) Affected by seawater intrusion, groundwater may not be suitable for irrigation, mainly due to high salinity and high hardness. When the Cl^- concentration is greater than 7.1 meq/L, groundwater will corrode pipelines and instruments. When the Cl^- concentration is greater than 14.1 meq/L, the groundwater hardness is too high, which may make the groundwater unsuitable for cultivation. When the Cl^- concentration is greater than 28.2 meq/L, excessively high salinity of groundwater will have adverse effects on planting. The areas affected by seawater intrusion should actively take measures to curb the intensification of seawater intrusion to maintain the sustainable development of local society and economy.

Author Contributions: Conceptualization, Z.W. and S.W.; methodology, Z.W.; software, Z.W. and S.W.; validation, S.W., Q.S., and W.L.; formal analysis, Z.W.; investigation, Z.W., S.W., W.L., Q.S., and H.T.; resources, Q.S., X.X., and Z.G.; data curation, Z.W. and J.L.; writing—original draft preparation, Z.W. and S.W.; writing—review and editing, W.L. and H.T.; supervision, Q.S., X.X., and Z.G.; project administration, X.X.; funding acquisition, Q.S. and X.X. All authors have read and agreed to the published version of the manuscript.

Funding: This research was funded by the First Institute of Oceanography, grant number “National Natural Science Foundation of China (U1806212)” and “Basic Scientific Fund for National Public Research (2020Q03)”.

Acknowledgments: The authors give their most sincere thanks to the editors and reviewers for their contributions to the improvement of this article.

Conflicts of Interest: The authors declare no conflict of interest.

Appendix A

Table A1. Testing results of groundwater samples.

Sample	Location	T (°C)	EC	TDS	pH	Na ⁺	K ⁺	Ca ²⁺	Mg ²⁺	Cl ⁻	SO ₄ ²⁻	HCO ₃ ⁻	Br ⁻
S01	Shouguang	22.50	5.88	4030.00	7.02	794.49	3.09	138.39	221.11	1467.56	557.85	396.07	2.75
S02	Shouguang	18.60	5.39	4030.00	6.85	1041.12	7.62	44.96	112.65	1606.18	239.26	530.13	3.65
H01	Hanting	17.80	1.92	1449.50	6.69	58.20	0.93	113.94	58.87	153.33	52.41	347.33	0.16
H02	Hanting	15.40	1.08	858.00	6.48	158.49	1.19	137.98	96.82	413.57	87.33	450.92	0.20
H03	Hanting	15.60	1.24	988.00	6.42	99.74	1.65	98.90	73.48	201.35	59.61	517.94	0.27
H04	Hanting	15.80	1.65	1306.50	6.35	171.28	3.33	142.59	67.32	162.90	117.04	505.76	0.24
H05	Hanting	14.50	5.65	4608.50	6.30	842.97	9.34	286.55	223.94	1679.22	412.59	584.97	2.73
H06	Hanting	19.40	3.37	2450.50	6.56	678.87	2.37	80.73	45.35	401.76	418.95	999.33	0.88
H07	Hanting	17.90	4.30	3237.00	6.37	749.91	6.24	271.29	116.46	1208.71	433.53	834.80	1.97
H08	Hanting	18.50	10.45	7767.50	6.50	1643.10	32.07	596.93	242.73	3222.22	1127.08	682.47	5.81
H09	Hanting	13.00	1.47	1235.00	6.43	216.41	0.68	63.61	67.30	150.84	147.24	444.82	0.17
H10	Hanting	12.70	1.56	1326.00	6.51	131.95	0.91	139.41	80.03	181.41	112.35	280.30	0.11
H11	Hanting	18.30	5.04	3757.00	6.47	786.86	5.91	218.87	148.21	1194.13	548.17	444.82	1.93
H12	Hanting	15.10	5.31	4270.50	6.50	988.89	7.76	77.08	189.39	1515.83	537.91	536.22	1.94
H13	Hanting	15.10	1.20	955.50	6.76	219.77	0.71	37.38	38.98	123.77	97.02	457.01	0.14
C01	Changyi	16.80	4.86	3744.00	6.80	1016.12	38.10	32.33	64.37	1463.37	200.07	487.48	2.95
C02	Changyi	16.50	3.74	2899.00	6.58	576.77	18.31	188.29	97.23	740.64	525.38	566.69	1.43
C03	Changyi	14.80	2.78	2249.00	6.64	460.62	20.59	112.90	71.35	574.68	349.11	310.77	0.72
C04	Changyi	16.20	1.71	1332.50	6.55	189.73	18.59	134.23	73.13	188.35	242.16	475.29	0.12
C05	Changyi	14.20	4.57	3750.50	6.21	1151.08	28.31	46.70	65.16	1023.94	728.92	907.93	1.15
C06	Changyi	16.20	2.35	1898.00	6.11	408.65	10.20	124.37	54.70	551.41	293.71	292.49	0.74
C07	Changyi	15.40	0.73	5785.00	6.61	41.17	1.41	99.73	18.23	116.80	77.54	255.93	0.08
C08	Changyi	14.80	2.18	1761.50	6.36	199.83	0.87	134.07	133.86	466.56	108.06	396.07	0.69
C09	Changyi	15.80	1.02	806.00	6.59	37.73	1.01	136.56	38.34	87.10	53.28	207.18	0.14
P01	Pingdu	15.00	4.63	3744.00	6.37	518.81	29.88	334.28	216.58	1375.38	581.81	554.50	1.82
P02	Pingdu	14.30	3.63	2977.00	6.54	450.29	40.66	221.71	154.77	971.94	554.35	304.67	1.63
P03	Pingdu	15.00	5.99	4823.00	6.43	975.70	35.69	306.57	194.11	1621.67	1022.47	511.85	1.59
P04	Pingdu	14.20	4.87	4017.00	6.48	582.38	46.96	302.82	271.60	1975.69	199.00	389.98	3.66
P05	Pingdu	15.30	2.43	1943.50	6.49	332.72	12.74	137.65	75.68	611.01	258.77	255.93	0.34

Table A1. Cont.

Sample	Location	T (°C)	EC	TDS	pH	Na ⁺	K ⁺	Ca ²⁺	Mg ²⁺	Cl ⁻	SO ₄ ²⁻	HCO ₃ ⁻	Br ⁻
P06	Pingdu	15.10	2.11	1696.50	6.39	187.88	3.74	200.63	79.82	402.21	89.50	383.89	0.42
P07	Pingdu	13.60	4.28	3568.50	6.49	877.15	7.01	126.45	101.63	1178.07	506.45	536.22	1.62
P08	Pingdu	17.40	2.15	1631.50	6.66	315.39	21.53	128.84	47.87	385.74	200.49	493.57	0.57
L01	Laizhou	14.30	1.19	968.50	6.22	50.93	1.20	207.20	23.35	169.08	82.07	292.49	0.12
L02	Laizhou	14.10	1.18	976.00	6.22	45.81	1.20	207.99	22.79	186.68	68.93	402.17	0.14
L03	Laizhou	14.20	1.44	1176.50	6.26	57.19	1.17	252.34	28.04	277.03	65.99	207.18	0.28
L04	Laizhou	14.90	1.60	1287.00	6.29	83.71	0.72	254.53	30.98	284.32	61.11	152.34	0.25
L05	Laizhou	21.90	2.54	1748.50	6.52	177.42	1.34	291.72	49.21	515.41	91.75	207.18	0.78
L06	Laizhou	16.40	1.94	1521.00	6.36	78.25	1.16	292.91	57.85	457.18	117.92	280.30	0.58
L07	Laizhou	14.70	1.02	832.00	6.56	38.53	0.87	161.88	28.74	151.61	84.92	213.27	0.08
L08	Laizhou	13.90	1.47	1222.00	6.48	49.06	1.15	267.38	36.02	184.86	126.06	225.46	0.24
L09	Laizhou	14.30	1.65	1358.50	6.59	52.13	4.75	291.39	47.39	288.69	103.06	207.18	0.22
L10	Laizhou	13.20	1.73	1443.00	6.51	79.21	1.05	274.37	60.51	367.82	143.36	292.49	0.28
L11	Laizhou	14.10	1.54	1274.00	6.55	162.48	1.76	195.84	32.54	176.57	130.45	243.74	0.17
L12	Laizhou	12.40	1.12	962.00	6.52	45.41	2.07	170.58	58.90	148.64	87.86	280.30	0.19

The units of TDS, Na⁺, K⁺, Ca²⁺, Mg²⁺, Cl⁻, SO₄²⁻, HCO₃⁻, Br⁻ are mg/L, and the unit of EC is ms/cm.

References

- Appelo, C.A.J.; Postma, D. *Geochemistry, Groundwater and Pollution*; CRC Press: Boca Raton, FL, USA, 2004.
- Todd, D.K.; Mays, L.W. *Groundwater Hydrology*; John Wiley & Sons: Hoboken, NJ, USA, 2004.
- Wang, S.; Gao, Z.; Wang, Z.; Wu, X.; An, Y.; Ren, X.; He, M.; Wang, W.; Liu, J. Hydrodynamic characteristics of groundwater aquifer system under recharge and discharge conditions. *Arab. J. Geosci.* **2020**, *13*, 1–12. [[CrossRef](#)]
- Merkel, B.J.; Planer-Friedrich, B.; Nordstrom, D.K. Groundwater Geochemistry. In *A Practical Guide to Modeling of Natural and Contaminated Aquatic Systems*; Springer: Berlin, Germany, 2005; p. 2.
- Matthess, G.; Frimmel, F.; Hirsch, P.; Schulz, H.; Usdowski, H. *Progress in Hydrogeochemistry: Organics, Carbonate Systems, Silicate Systems, Microbiology, Models*; Springer: Berlin, Germany, 1992.
- Gao, Z.; Wang, Z.; Wang, S.; Wu, X.; An, Y.; Wang, W.; Liu, J. Factors that influence the chemical composition and evolution of shallow groundwater in an arid region: A case study from the middle reaches of the Heihe River, China. *Environ. Earth Sci.* **2019**, *78*, 390. [[CrossRef](#)]
- Fitts, C.R. *Groundwater Science*; Elsevier: Amsterdam, The Netherlands, 2002.
- Famiglietti, J.S. The global groundwater crisis. *Nat. Clim. Chang.* **2014**, *4*, 945–948. [[CrossRef](#)]
- Liu, J.; Gao, Z.; Wang, Z.; Xu, X.; Su, Q.; Wang, S.; Qu, W.; Xing, T. Hydrogeochemical processes and suitability assessment of groundwater in the Jiaodong Peninsula, China. *Environ. Monit. Assess.* **2020**, *192*, 384. [[CrossRef](#)] [[PubMed](#)]
- Bear, J.; Cheng, A.H.-D.; Sorek, S.; Ouazar, D.; Herrera, I. *Seawater Intrusion in Coastal Aquifers: Concepts, Methods and Practices*; Springer Science & Business Media: Berlin, Germany, 1999.
- Mahmoodzadeh, D.; Karamouz, M. Seawater intrusion in heterogeneous coastal aquifers under flooding events. *J. Hydrol.* **2019**, *568*, 1118–1130. [[CrossRef](#)]
- Badaruddin, S.; Werner, A.D.; Morgan, L.K. Characteristics of active seawater intrusion. *J. Hydrol.* **2017**, *551*, 632–647. [[CrossRef](#)]
- Xiao, H.; Wang, D.; Medeiros, S.C.; Bilskie, M.V.; Hagen, S.C.; Hall, C.R. Exploration of the effects of storm surge on the extent of saltwater intrusion into the surficial aquifer in coastal east-central Florida (USA). *Sci. Total Environ.* **2019**, *648*, 1002–1017. [[CrossRef](#)]
- Parizi, E.; Hosseini, S.M.; Ataie-Ashtiani, B.; Simmons, C.T. Vulnerability mapping of coastal aquifers to seawater intrusion: Review, development and application. *J. Hydrol.* **2019**, *570*, 555–573. [[CrossRef](#)]
- Arsilan, H.; Demir, Y. Impacts of seawater intrusion on soil salinity and alkalinity in Bafra Plain, Turkey. *Environ. Monit. Assess.* **2013**, *185*, 1027–1040. [[CrossRef](#)]
- Hussain, M.S.; Abd-Elhamid, H.F.; Javadi, A.A.; Sherif, M.M. Management of seawater intrusion in coastal aquifers: A review. *Water* **2019**, *11*, 2467. [[CrossRef](#)]
- Shi, W.; Lu, C.; Ye, Y.; Wu, J.; Li, L.; Luo, J. Assessment of the impact of sea-level rise on steady-state seawater intrusion in a layered coastal aquifer. *J. Hydrol.* **2018**, *563*, 851–862. [[CrossRef](#)]
- Herzberg, A. Die Wasserversorgung einiger Nordseebäder: Journal für Gasbeleuchtung und Wasserversorgung. *J. Hydrol.* **2018**, *26*, 1789–1799.
- Luyun Jr, R.; Momii, K.; Nakagawa, K. Effects of recharge wells and flow barriers on seawater intrusion. *Groundwater* **2011**, *49*, 239–249. [[CrossRef](#)] [[PubMed](#)]
- Abd-Elhamid, H.; Javadi, A.; Abdelaty, I.; Sherif, M. Simulation of seawater intrusion in the Nile Delta aquifer under the conditions of climate change. *Hydrol. Res.* **2016**, *47*, 1198–1210. [[CrossRef](#)]
- Shi, W.; Lu, C.; Werner, A.D. Assessment of the impact of sea-level rise on seawater intrusion in sloping confined coastal aquifers. *J. Hydrol.* **2020**, *586*, 124872. [[CrossRef](#)]
- Liu, S.; Tang, Z.; Gao, M.; Hou, G. Evolutionary process of saline-water intrusion in Holocene and Late Pleistocene groundwater in southern Laizhou Bay. *Sci. Total Environ.* **2017**, *607*, 586–599. [[CrossRef](#)] [[PubMed](#)]
- Chen, Q.; Wei, J.; Wang, H.; Shi, L.; Gao, Z.; Liu, S.; Ning, F.; Jia, C.; Ji, Y.; Dong, F. Discussion on the fluorosis in seawater-intrusion areas along coastal zones in Laizhou Bay and other parts of China. *Int. J. Environ. Res.* **2019**, *13*, 435–442. [[CrossRef](#)]

24. Qi, H.; Ma, C.; He, Z.; Hu, X.; Gao, L. Lithium and its isotopes as tracers of groundwater salinization: A study in the southern coastal plain of Laizhou Bay, China. *Sci. Total Environ.* **2019**, *650*, 878–890. [[CrossRef](#)]
25. Al Maliki, A.A.; Abbass, Z.D.; Hussain, H.M.; Al-Ansari, N. Assessment of the groundwater suitability for irrigation near Al Kufa City and preparing the final water quality maps using spatial distribution tools. *Environ. Earth Sci.* **2020**, *79*, 1–12. [[CrossRef](#)]
26. Jeon, C.; Raza, M.; Lee, J.-Y.; Kim, H.; Kim, C.-S.; Kim, B.; Kim, J.-W.; Kim, R.-H.; Lee, S.-W. Countrywide Groundwater Quality Trend and Suitability for Use in Key Sectors of Korea. *Water* **2020**, *12*, 1193. [[CrossRef](#)]
27. Piper, A. A Graphic Procedure in the Geochemical Interpretation of Water-Analyses. *Neurochem. Int.* **1984**, *6*, 27–39. [[CrossRef](#)]
28. Gibbs, R.J. Mechanisms controlling world water chemistry. *Science* **1970**, *170*, 1088–1090. [[CrossRef](#)] [[PubMed](#)]
29. Mahanta, N.; Mishra, I.; Hatui, A.; Mahanta, P.; Sahoo, H.; Goswami, S. Geochemical appraisal of groundwater qualities and its uses in and around Maneswar Block of Sambalpur District, Odisha, India. *Environ. Earth Sci.* **2020**, *79*, 5. [[CrossRef](#)]
30. Rao, N.S. Controlling factors of fluoride in groundwater in a part of South India. *Arab. J. Geosci.* **2017**, *10*, 524.
31. Richard, L. *Diagnosis and Improvement of Saline and Alkali Soils*. USDA Hand Book. No. 60; US Government Press: Washington, DC, USA, 1954; p. 160.
32. Wilcox, L. *Classification and Use of Irrigation Waters*; US Department of Agriculture: Washington, DC, USA, 1955.
33. Raman, V. Impact of corrosion in the conveyance and distribution of water. *J. Indian Water Works Assoc.* **1983**, *15*, 115–121.
34. Tomaszewicz, M.; Abou Najm, M.; El-Fadel, M. Development of a groundwater quality index for seawater intrusion in coastal aquifers. *Environ. Model. Softw.* **2014**, *57*, 13–26. [[CrossRef](#)]
35. Khan, A.F.; Srinivasamoorthy, K.; Prakash, R.; Rabina, C. Hydrochemical and statistical techniques to decode groundwater geochemical interactions and saline water intrusion along the coastal regions of Tamil Nadu and Puducherry, India. *Environ. Geochem. Health* **2020**, 1–17. [[CrossRef](#)]
36. Sae-Ju, J.; Chotpanarat, S.; Thitimakorn, T. Assessment of seawater intrusion using multivariate statistical, hydrochemical and geophysical techniques in coastal aquifer, Cha-am district, Thailand. *Hydrol. Earth Syst. Sci. Discuss.* **2018**, 1–50. [[CrossRef](#)]
37. Papatheodorou, G.; Lambrakis, N.; Panagopoulos, G. Application of multivariate statistical procedures to the hydrochemical study of a coastal aquifer: An example from Crete, Greece. *Hydrol. Process. Int. J.* **2007**, *21*, 1482–1495. [[CrossRef](#)]
38. Sridharan, M.; Nathan, D.S. Hydrochemical facies and ionic exchange in coastal aquifers of Puducherry region, India: Implications for seawater intrusion. *Earth Syst. Environ.* **2017**, *1*, 5. [[CrossRef](#)]
39. Lee, J.-Y.; Song, S.-H. Groundwater chemistry and ionic ratios in a western coastal aquifer of Buan, Korea: Implication for seawater intrusion. *Geosci. J.* **2007**, *11*, 259–270. [[CrossRef](#)]
40. Park, S.-C.; Yun, S.-T.; Chae, G.-T.; Yoo, I.-S.; Shin, K.-S.; Heo, C.-H.; Lee, S.-K. Regional hydrochemical study on salinization of coastal aquifers, western coastal area of South Korea. *J. Hydrol.* **2005**, *313*, 182–194. [[CrossRef](#)]
41. Han, D.; Kohfahl, C.; Song, X.; Xiao, G.; Yang, J. Geochemical and isotopic evidence for palaeo-seawater intrusion into the south coast aquifer of Laizhou Bay, China. *Appl. Geochem.* **2011**, *26*, 863–883. [[CrossRef](#)]
42. Kharroubi, A.; Tlahigue, F.; Agoubi, B.; Azri, C.; Bouri, S. Hydrochemical and statistical studies of the groundwater salinization in Mediterranean arid zones: Case of the Jerba coastal aquifer in southeast Tunisia. *Environ. Earth Sci.* **2012**, *67*, 2089–2100. [[CrossRef](#)]
43. Davis, S.N.; Whittemore, D.O.; Fabryka-Martin, J. Uses of chloride/bromide ratios in studies of potable water. *Groundwater* **1998**, *36*, 338–350. [[CrossRef](#)]
44. Han, D.M.; Song, X.F.; Currell, M.J.; Yang, J.L.; Xiao, G.Q. Chemical and isotopic constraints on evolution of groundwater salinization in the coastal plain aquifer of Laizhou Bay, China. *J. Hydrol.* **2014**, *508*, 12–27. [[CrossRef](#)]
45. Chafouq, D.; El Mandour, A.; Elgettafi, M.; Himi, M.; Chouikri, I.; Casas, A. Hydrochemical and isotopic characterization of groundwater in the Ghis-Nekor plain (northern Morocco). *J. Afr. Earth Sci.* **2018**, *139*, 1–13. [[CrossRef](#)]
46. Terzić, J.; Marković, T.; Pekaš, Ž. Influence of sea-water intrusion and agricultural production on the Blato Aquifer, Island of Korčula, Croatia. *Environ. Geol.* **2008**, *54*, 719–729. [[CrossRef](#)]

47. Sappa, G.; Ergul, S.; Ferranti, F.; Sweya, L.N.; Luciani, G. Effects of seasonal change and seawater intrusion on water quality for drinking and irrigation purposes, in coastal aquifers of Dar es Salaam, Tanzania. *J. Afr. Earth Sci.* **2015**, *105*, 64–84. [[CrossRef](#)]
48. Milnes, E.; Renard, P. The problem of salt recycling and seawater intrusion in coastal irrigated plains: An example from the Kiti aquifer (Southern Cyprus). *J. Hydrol.* **2004**, *288*, 327–343. [[CrossRef](#)]
49. Abdoulhalik, A.; Ahmed, A.; Hamill, G. A new physical barrier system for seawater intrusion control. *J. Hydrol.* **2017**, *549*, 416–427. [[CrossRef](#)]
50. Nishikawa, T.; Siade, A.J.; Reichard, E.G.; Ponti, D.J.; Canales, A.; Johnson, T. Stratigraphic controls on seawater intrusion and implications for groundwater management, Dominguez Gap area of Los Angeles, California, USA. *Hydrogeol. J.* **2009**, *17*, 1699. [[CrossRef](#)]

Publisher's Note: MDPI stays neutral with regard to jurisdictional claims in published maps and institutional affiliations.



© 2020 by the authors. Licensee MDPI, Basel, Switzerland. This article is an open access article distributed under the terms and conditions of the Creative Commons Attribution (CC BY) license (<http://creativecommons.org/licenses/by/4.0/>).